Supplementary Information

Energetic Copper(II) Quadridentate Chelate: A Novel Green Laser-sensitive Primary Explosive

Qi Zhang,*[a] Ruibing Lv,[a] Ying Wang,[a] Zhenghang Luo,[a] Pengyang Pan,[a] Tingwei Wang[a] and Quancheng Liu *[b]

[a] Institute of Chemical Materials, China Academy of Engineering Physics (CAEP), Mianyang 621900, P. R. China.
[b] School of Information Engineering, Southwest University of Science and Technology, Mianyang 621010, P. R. China.

Corresponding author: Qi Zhang, Quancheng Liu
E-mail: jackzhang531@ caep.cn (Q. Zhang); liuqc@swust.edu.cn (Q. Liu).

Table of Contents

1. IR Curves

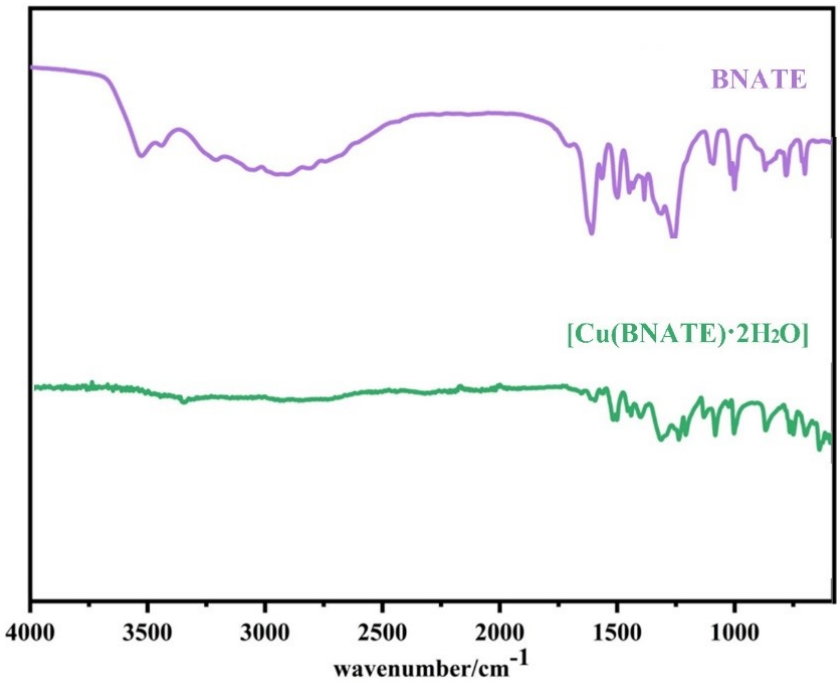

Figure S1. IR Curves of BNATE and [Cu(BNATE)·2H_2O] (1)

2. Powder X-ray diffraction (PXRD) spectra

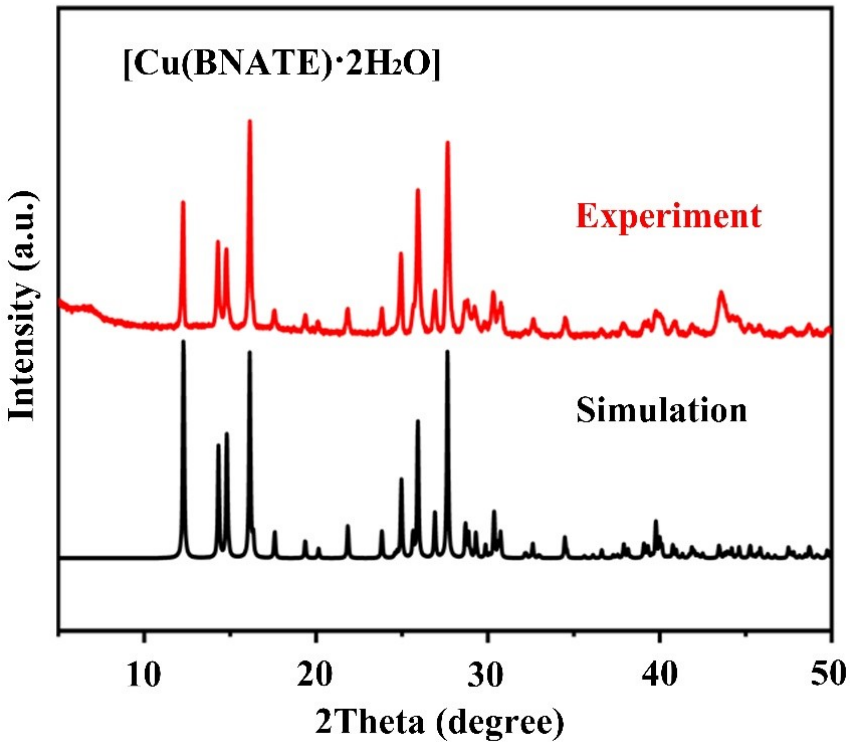

Figure S2. PXRD spectra of [Cu(BNATE)·2H_2O] (1)

3. X-ray Crystallography

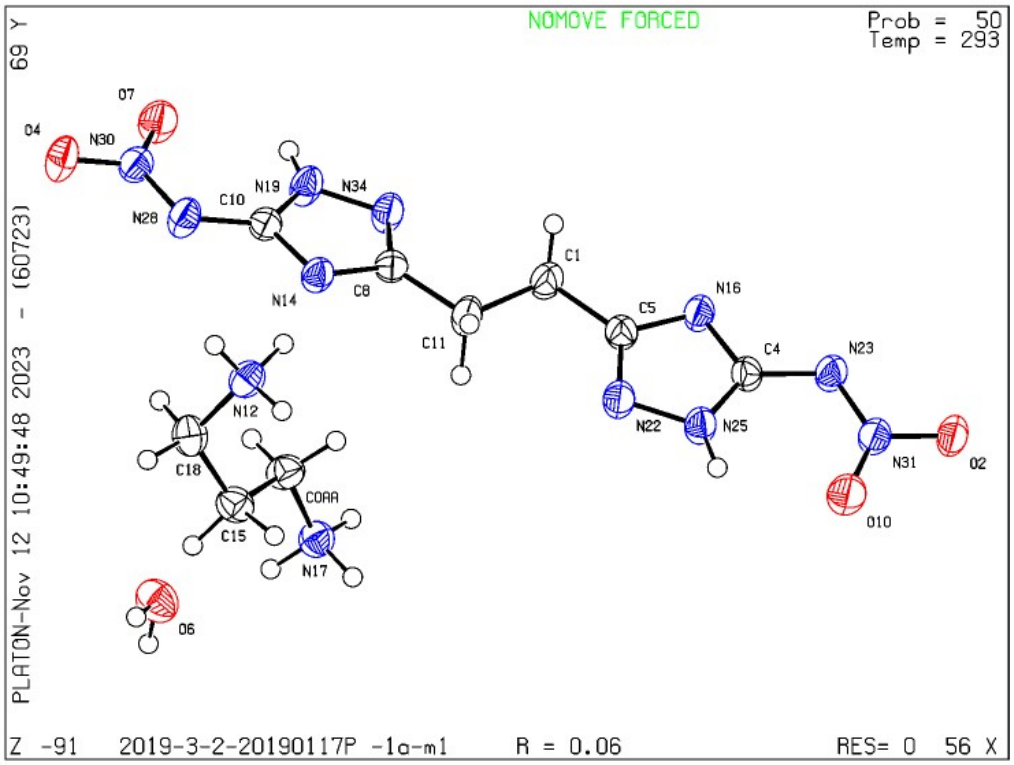

Figure S3. The asymmetric unit of BNATE-DAP[1]

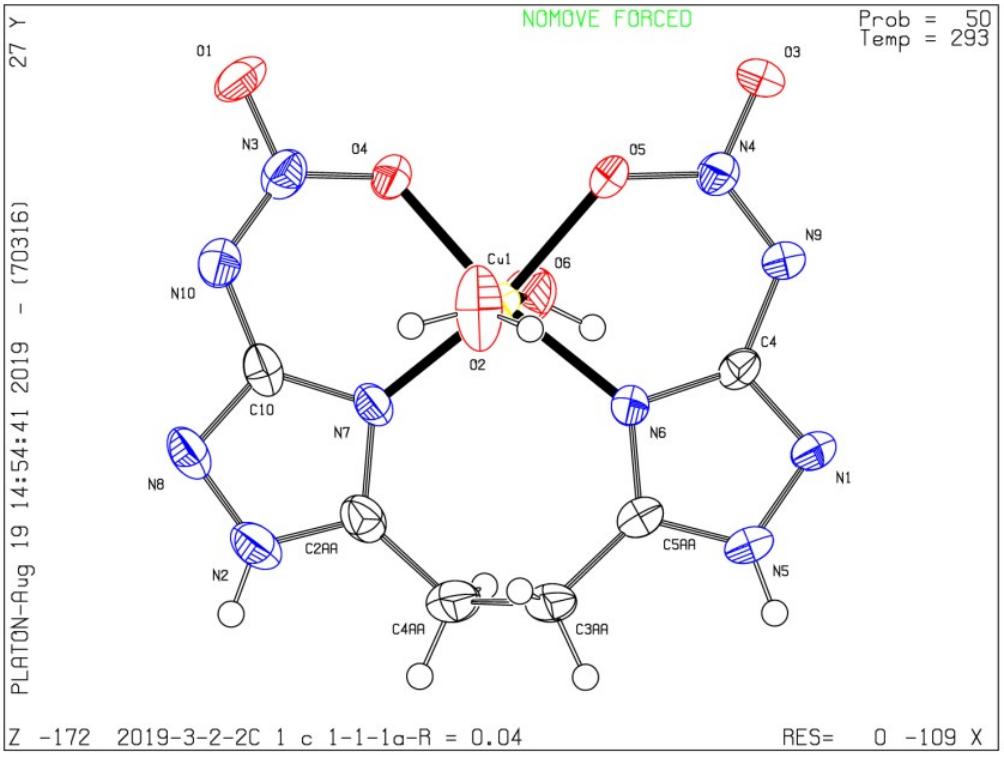

Figure S4. The asymmetric unit of [Cu(BNATE)·2H_2O] (1)

Table S1 Crystal data and structure refinement for [Cu(BNATE)·2H_2O] and BNATE-DAP.

Compounds	[Cu(BNATE)·2H_2O] (1)	BNATE-DAP
CCDC number	2313137	2313138
Empirical formula	$C_6H_{10}CuN_{10}O_6$	$C_9H_{20}N_{12}O_5$
Formula weight	381.78	376.37
Temperature/K	293.15	293.15
Crystal system	monoclinic	triclinic
Space group	Cc	P-1
a/Å	7.3292(4)	7.7570(9)
b/Å	11.8696(8)	8.0095(6)
c/Å	14.5806(8)	13.8397(11)
α/°	90	99.700(6)
β/°	99.093(5)	102.391(8)
γ/°	90	102.769(8)
Volume/Å^3	1252.49(13)	797.74(13)
Z	4	2
ρ_{calc}g/cm^3	2.025	1.567
μ/mm^{-1}	1.803	0.129
F(000)	772.0	396.0
Radiation	MoKα (λ = 0.71073)	MoKα (λ = 0.71073)
2Θ range for data collection/°	7.426 to 57.894	7.168 to 57.898
Index ranges	-9 ≤ h ≤ 5, -8 ≤ k ≤ 15, -18 ≤ l ≤ 19	-10 ≤ h ≤ 6, -10 ≤ k ≤ 10, -18 ≤ l ≤ 18
Reflections collected	2407	5792
Independent reflections	1970 [R_{int} = 0.0226, R_{sigma} = 0.0535]	3611 [R_{int} = 0.0258, R_{sigma} = 0.0655]
Data/restraints/parameters	1970/2/209	3611/0/315
Goodness-of-fit on F^2	1.085	1.039
Final R indexes [I>=2σ (I)]	R_1 = 0.0382, wR_2 = 0.0850	R1 = 0.0570, wR2 = 0.1126
Final R indexes [all data]	R_1 = 0.0408, wR_2 = 0.0886	R1 = 0.1005, wR2 = 0.1396
Largest diff. peak/hole / e Å^{-3}	0.43/-0.41	0.22/-0.26

Table S2 Selected bond lengths [Å] for [Cu(BNATE)·2H_2O].

Atom	Atom	Length/Å	Atom	Atom	Length/Å
Cu1	O2	2.397(6)	N3	N10	1.307(8)
Cu1	O4	1.982(4)	N4	N9	1.290(7)
Cu1	O5	1.965(5)	N5	C5	1.331(7)
Cu1	O6	2.331(5)	N6	C6	1.368(7)
Cu1	N6	1.967(5)	N6	C5	1.331(8)
Cu1	N7	1.941(5)	N7	C2	1.359(8)
O1	N3	1.240(6)	N7	C1	1.377(7)
O3	N4	1.245(7)	N8	C1	1.319(8)
O4	N3	1.295(6)	N9	C6	1.387(8)
O5	N4	1.290(6)	N10	C1	1.371(8)
N1	N5	1.357(7)	C2	C4	1.470(10)
N1	C6	1.308(7)	C3	C4	1.538(9)
N2	N8	1.365(8)	C3	C5	1.479(9)
N2	C2	1.316(8)			

Table S3 Selected bond Angles [°] for [Cu(BNATE)·2H_2O].

Atom	Atom	Atom	Angle/°	Atom	Atom	Atom	Angle/°
O4	Cu1	O2	93.6(2)	C5	N5	N1	110.5(5)
O4	Cu1	O6	87.4(2)	C6	N6	Cu1	121.6(4)
O5	Cu1	O2	89.8(2)	C5	N6	Cu1	134.0(4)
O5	Cu1	O4	82.79(19)	C5	N6	C6	103.7(5)
O5	Cu1	O6	89.2(2)	C2	N7	Cu1	133.9(4)
O5	Cu1	N6	87.4(2)	C2	N7	C1	102.8(5)
O6	Cu1	O2	178.44(19)	C1	N7	Cu1	122.9(4)
N6	Cu1	O2	87.4(2)	C1	N8	N2	101.9(5)
N6	Cu1	O4	170.1(2)	N4	N9	C6	120.1(5)
N6	Cu1	O6	91.41(19)	N3	N10	C10	120.7(5)
N7	Cu1	O2	87.1(2)	N2	C2	N7	108.5(6)
N7	Cu1	O4	87.1(2)	N2	C2	C4	123.9(6)
N7	Cu1	O5	169.2(2)	N7	C2	C4	127.6(6)
N7	Cu1	O6	94.1(2)	C5	C3	C4	115.1(6)
N7	Cu1	N6	102.8(2)	N1	C6	N6	113.6(6)
N3	O4	Cu1	129.7(4)	N1	C6	N9	115.5(5)
N4	O5	Cu1	131.3(4)	N6	C6	N9	130.9(5)
C6	N1	N5	103.3(5)	C2	C4	C3	115.5(6)
C2	N2	N8	112.3(5)	N5	C5	N6	109.0(6)
O1	N3	O4	116.0(5)	N5	C5	C3	122.2(5)

O1	N3	N10	118.9(5)	N6	C5	C3	128.8(5)
O4	N3	N10	125.1(5)	N8	C1	N7	114.4(6)
O3	N4	O5	115.4(5)	N8	C1	N10	115.6(5)
O3	N4	N9	118.7(5)	N10	C1	N7	130.0(6)
O5	N4	N9	125.9(5)				

Table S4 Selected torsion Angles [°] for [Cu(BNATE)·2H_2O].

A	**B**	**C**	**D**	**Angle/°**
Cu1	O4	N3	O1	164.4(5)
Cu1	O4	N3	N10	-17.4(9)
Cu1	O5	N4	O3	171.1(5)
Cu1	O5	N4	N9	-9.9(10)
Cu1	N6	C6	N1	-170.1(4)
Cu1	N6	C6	N9	11.7(8)
Cu1	N6	C5	N5	168.8(5)
Cu1	N6	C5	C3	-13.4(11)
Cu1	N7	C2	N2	171.0(4)
Cu1	N7	C2	C4	-10.8(10)
Cu1	N7	C1	N8	-171.9(4)
Cu1	N7	C1	N10	8.0(9)
O1	N3	N10	C1	176.2(6)
O3	N4	N9	C6	175.7(5)
O4	N3	N10	C1	-2.0(9)
O5	N4	N9	C6	-3.3(9)
N1	N5	C5	N6	0.9(7)
N1	N5	C5	C3	-177.1(6)
N2	N8	C1	N7	-1.1(7)
N2	N8	C1	N10	179.0(5)
N2	C2	C4	C3	-122.6(7)
N3	N10	C1	N7	6.6(10)
N3	N10	C1	N8	-173.5(5)
N4	N9	C6	N1	-176.5(5)
N4	N9	C6	N6	1.7(9)
N5	N1	C6	N6	-1.2(7)
N5	N1	C6	N9	177.4(5)
N7	C2	C4	C3	59.5(9)
N8	N2	C2	N7	1.0(7)
N8	N2	C2	C4	-177.2(6)
C2	N2	N8	C1	0.1(7)
C2	N7	C1	N8	1.7(7)
C2	N7	C1	N10	-178.4(6)
C6	N1	N5	C5	0.1(7)
C6	N6	C5	N5	-1.5(7)

C6	N6	C5	C3	176.3(7)
C4	C3	C5	N5	-125.9(7)
C4	C3	C5	N6	56.5(10)
C5	N6	C6	N1	1.7(7)
C5	N6	C6	N9	-176.5(6)
C5	C3	C4	C2	-83.6(8)
C1	N7	C2	N2	-1.5(7)
C1	N7	C2	C4	176.6(6)

Table S5 Selected bond lengths [Å] for BNATE-DAP.

Atom	**Atom**	**Length/Å**	**Atom**	**Atom**	**Length/Å**
O2	N31	1.282(2)	N22	C5	1.313(3)
O4	N30	1.275(2)	N23	N31	1.305(3)
O7	N30	1.246(2)	N23	C4	1.380(3)
O10	N31	1.238(2)	N25	C4	1.333(3)
N12	C18	1.482(3)	N28	N30	1.306(3)
N14	C8	1.365(3)	N28	C10	1.374(3)
N14	C10	1.335(3)	N34	C8	1.320(3)
N16	C4	1.332(3)	C1	C5	1.492(3)
N16	C5	1.364(3)	C1	C11	1.499(3)
N17	C0AA	1.475(3)	C8	C11	1.494(3)
N19	N34	1.372(3)	C0AA	C15	1.510(3)
N19	C10	1.336(3)	C15	C18	1.510(4)
N22	N25	1.370(3)			

Table S6 Selected bond Angles [°] for BNATE-DAP.

Atom	**Atom**	**Atom**	**Angle/ °**	**Atom**	**Atom**	**Atom**	**Angle/ °**
C10	N14	C8	103.96(18)	N16	C4	N25	109.58(19)
C4	N16	C5	103.51(18)	N25	C4	N23	131.7(2)
C10	N19	N34	110.24(18)	N16	C5	C1	122.1(2)
C5	N22	N25	102.87(17)	N22	C5	N16	114.1(2)
N31	N23	C4	116.55(19)	N22	C5	C1	123.8(2)
C4	N25	N22	109.94(18)	N14	C8	C11	121.9(2)
N30	N28	C10	117.11(19)	N34	C8	N14	113.81(19)
O4	N30	N28	115.46(19)	N34	C8	C11	124.2(2)
O7	N30	O4	119.99(18)	N14	C10	N19	109.17(19)
O7	N30	N28	124.55(19)	N14	C10	N28	119.02(19)

Table S7 Selected torsion Angles [°] for BNATE-DAP.

A	**B**	**C**	**D**	**Angle/°**
N14	C8	C11	C1	-162.7(3)
N17	C0AA	C15	C18	-168.8(2)

N19	N34	C8	N14	-0.2(3)
N19	N34	C8	C11	177.8(3)
N22	N25	C4	N16	0.0(3)
N22	N25	C4	N23	179.5(3)
N25	N22	C5	N16	-0.9(3)
N25	N22	C5	C1	179.3(3)
N30	N28	C10	N14	177.5(2)
N30	N28	C10	N19	-1.6(4)
N31	N23	C4	N16	-176.1(2)
N31	N23	C4	N25	4.4(4)
N34	N19	C10	N14	0.6(3)
N34	N19	C10	N28	179.7(3)
N34	C8	C11	C1	19.5(4)
C4	N16	C5	N22	0.9(3)
C4	N16	C5	C1	-179.3(3)
C4	N23	N31	O2	178.3(2)
C4	N23	N31	O10	-2.0(4)
C5	N16	C4	N23	179.9(2)
C5	N16	C4	N25	-0.5(3)
C5	N22	N25	C4	0.5(3)
C5	C1	C11	C8	-178.2(3)
C8	N14	C10	N19	-0.7(3)
C8	N14	C10	N28	-179.9(2)
C10	N14	C8	N34	0.5(3)
C10	N14	C8	C11	-177.5(2)
C10	N19	N34	C8	-0.2(3)
C10	N28	N30	O4	-178.1(2)
C10	N28	N30	O7	2.5(4)
C11	C1	C5	N16	176.7(3)
C11	C1	C5	N22	-3.5(4)
C0AA	C15	C18	N12	-68.7(3)

4. Heats of formation calculations

The constant pressure reaction heat ($^{\Delta_c U}$) of chelate [Cu(BNATE)·2H_2O] (1) was measured by the oxygen bomb calorimeter, and the value of $^{\Delta_c U}$ is the average of three independent experiment results. Standard molar combustion enthalpy ($^{\Delta_c H_m^\theta}$) can be obtained from the constant pressure reaction heat ($^{\Delta_c U}$) and equation 2. The standard molar combustion enthalpy ($\Delta_f H$) of chelate [Cu(BNATE)·2H_2O] (-453 kJ mol^{-1}) was obtained from $^{\Delta_c H_m^\theta}$ according to equation 3. (CO_2(g): -393.51 kJ mol^{-1}; H_2O(l): 285.85 kJ mol^{-1}; CuO(s): -155.2 kJ mol^{-1})

$$C_6H_{10}CuN_{10}O_6\ (s)+6O_2(g)=6CO_2(g)+CuO(s)+5H_2O(l)+5N_2(g) \quad (1)$$

$$\Delta_c H_m^\theta = \Delta_c U + \Delta nRT \quad (2)$$

$$\Delta_f H_m^\theta = \sum \Delta_f H_m^\theta\,(products) - \Delta_c H_m^\theta \quad (3)$$

$\Delta n = {}^{n_g}$(products) - ^{n_g}(reactants), (^{n_g} is the sum of the total moles of gas in the product or reactant, R= 8.314 J mol^{-1} K^{-1}, T= 298.15 K)

5. Hole-electron and Interfragment Charge Transfer (IFCT) analysis

Gaussian16 software was used to perform geometric optimization on [Cu(BNATE)·2H_2O] based on B3LYP density functional and 6-311G* basis set, and the TD-DFT method was used to calculate its excited state and obtain its electronic transition properties. In addition, using Multiwfn and Multiwfn software, hole-electron analysis was performed on the specific excited state of [Cu(BNATE)·2H_2O]. Its distribution is shown in Figure S5, where blue is the hole region, green is the electronic area, that is, electrons transfer from the blue area to the green area during the transition. It can be seen from the contribution of atoms to holes and electrons that when electrons transition in the [Cu(BNATE)·2H_2O] molecule, 84.44% of holes and 68.58% of electrons are distributed on Cu2+, and other holes are mainly distributed on Cu^{2+} The other electrons are mainly distributed at the two nitro O atoms and two triazole N atoms participating in the coordination. Table S8 shows the hole and electron distribution percentages for each non-hydrogen atom position.

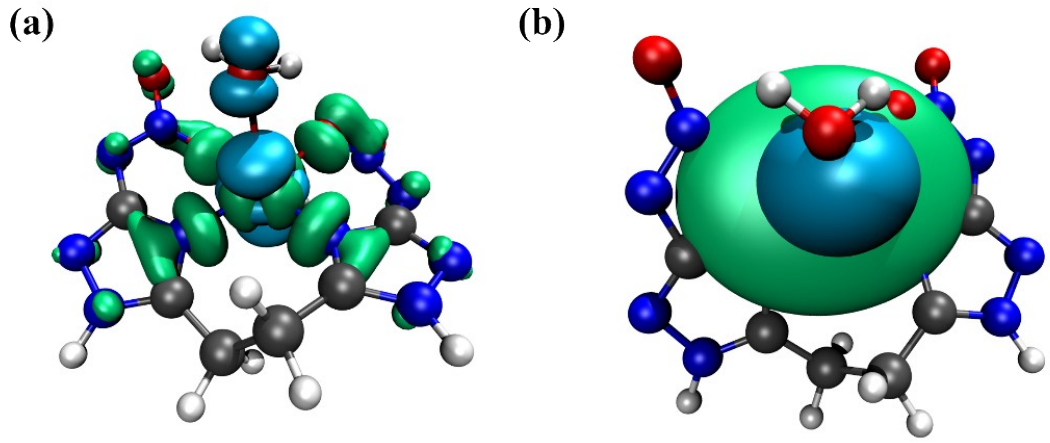

Figure S5. (a) Hole–electron distributions of [Cu(BNATE)·2H_2O]; (b) C_{ele} and C_{hole} in [Cu(BNATE)·2H_2O].

Table S8 Contribution of each non-hydrogen atom to hole and electron.

Atoms	Hole/%	Electron/%	Overlap/%	Diff/%
1(Cu)	84.44	68.58	76.1	-15.86
2(O)	0.33	0.96	0.56	0.64
3(O)	4.61	0.02	0.28	-4.59
6(O)	0.32	0.96	0.55	0.64
7(O)	1.78	5.83	3.22	4.06
8(O)	1.85	5.84	3.28	4
9(O)	4.52	0.02	0.28	-4.5
12(N)	0.03	0.46	0.12	0.43
13(N)	0.02	0.36	0.09	0.33
15(N)	0.06	0.47	0.17	0.41
16(N)	0.06	0.47	0.17	0.41
17(N)	0.02	0.36	0.09	0.33
19(N)	0.42	5.87	1.56	5.46
20(N)	0.42	5.86	1.57	5.44
21(N)	0.04	0.46	0.14	0.41
22(N)	0.17	0.86	0.39	0.69
23(N)	0.2	0.87	0.42	0.67
24(C)	0.13	0.37	0.22	0.24
25(C)	0.01	0.04	0.02	0.02
28(C)	-0.01	0.32	0	0.33
29(C)	0.01	0.04	0.02	0.02
32(C)	0.13	0.37	0.22	0.24
33(C)	-0.01	0.32	0	0.33
Sum	99.55	99.70	□	□

Use the IFCT (interfragment charge transfer) method of the Multiwfn program to quantitatively analyze the amount of electron transfer between each fragment of the molecule in a specific excited state transition, and use the electron density difference (CDD, charge density transfer) diagram between the excited state and the ground state (Fig. 4b), showing the electron density changes of each fragment in a visual form, and finally determining the electronic transition mode. The fragment division is shown in Figure S6, and the calculated electron transfer percentage of each fragment is shown in Table S9. Table S10 shows the Intrinsic charge transfer (CT) and local excitation (LE) percentage during the [Cu(BNATE)·2H_2O] excitation process. CT mode is further divided into metal-ligand charge transfer (MLCT, metal-ligand charge transfer), ligand-to-metal charge transfer (LMCT, ligand-metal charge transfer) and charge transfer between ligands (LLCT, ligand-ligand charge transfer), while the LE mode includes metal-centered transitions (MC, metal centered) and

intra-ligand or ligand-centered transitions (LC, ligand centered).

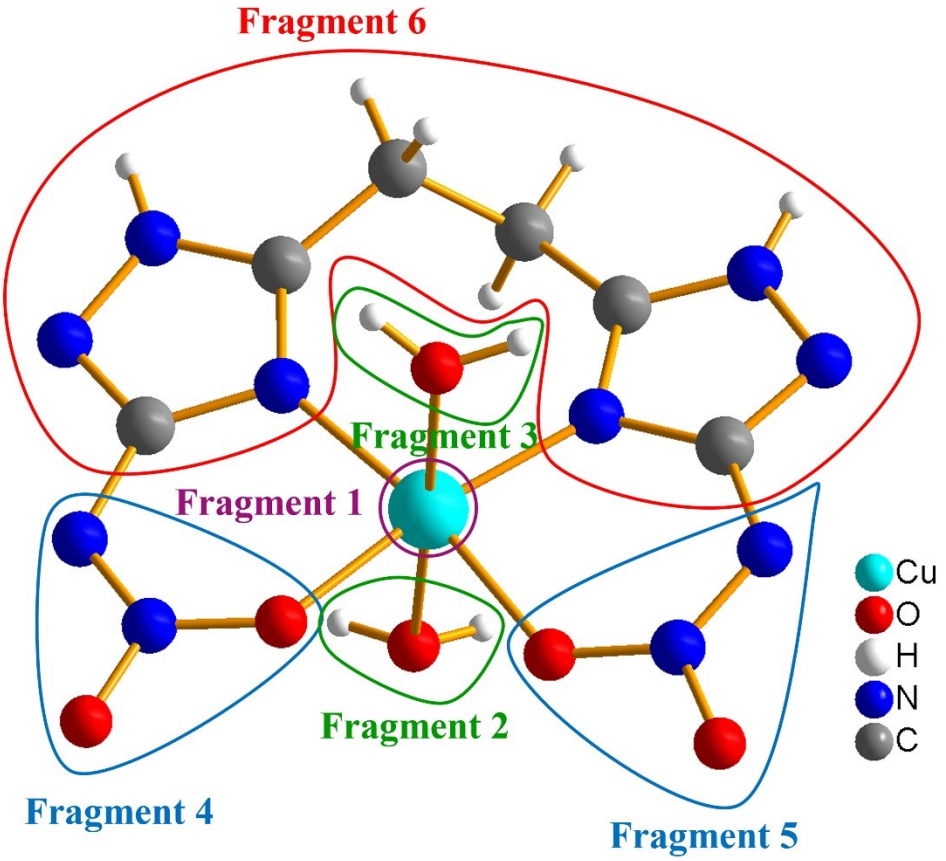

Figure S6. Fragments division of [Cu(BNATE)·2H_2O]

Table S9 Transferred electrons between fragments.

Donors[a]	Receptors[b]					
	Cu^{2+}	H_2O (1)	H_2O (2)	-NNO_2(1)	-NNO_2(2)	$C_6N_6H_6$
Cu^{2+}	0.57913	0.00053	0.00053	0.06868	0.06874	0.12682
H_2O (1)	0.03306	0.00003	0.00003	0.00392	0.00392	0.00724
H_2O (2)	0.03243	0.00003	0.00003	0.00385	0.00385	0.00710
-NNO_2 (1)	0.01620	0.00001	0.00001	0.00192	0.00192	0.00355
-NNO_2 (2)	0.01647	0.00002	0.00002	0.00195	0.00195	0.00361
$C_6N_6H_6$	0.00853	0.00001	0.00001	0.00101	0.00101	0.00187

[a] The molecular fragments that provide electrons during excitation; [b] The molecular fragments that receive electrons during excitation; The unit for all data in the table is ***e***.

Table S10. Intrinsic charge transfer (CT) and local excitation (LE) percentage.

CT (41.507 %)			LE (58.493 %)	
MLCT (e)	LMCT (e)	LLCT (e)	MC (e)	LC (e)
0.2653	0.10669	0.04307	0.57913	0.0058

6. References

1. P. Pan, T. Wang, Q. Zhang, S. Zhu and L. Zhang, Crystal and Properties of 1,2-Bis(3,3'-Dinitroamine-1H-1,2,4-Triazol-5-yl) ethane and Its 1,3-Propanediamine Salt, *Chinese Journal of Energetic Materials*, 2021, 29, 732–738.